

Effect of Abrikosov vortices on the critical current of a Josephson junction

V. N. Gubankov, M. P. Lisitskiĭ, I. L. Serpuchenko, and M. V. Fistul'

Institute of Radio Engineering and Electronics, Academy of Sciences of the USSR

(Submitted 23 April 1991)

Zh. Eksp. Teor. Fiz. **100**, 1326–1339 (October 1991)

The behavior of the critical current of a Josephson junction as a function of the concentration of pinned Abrikosov vortices of various types is studied theoretically. In related experiments, Abrikosov vortices were introduced into Josephson junctions based on niobium films in two ways: by cooling the junction through T_c in a magnetic field directed perpendicular to the plane of the junction, H_\perp , and by applying a field H_\perp after the junction had already reached a temperature $T < T_c$. When mismatched vortices are pinned, the maximum critical current I_c^{\max} falls off exponentially with increasing H_\perp . The curve of $I_c^{\max}(H_\perp)$ for isolated vortices has a characteristic inflection point. The $I_c^{\max}(H_\perp)$ curves found here can be used to determine the size of the mismatched vortices and to estimate the critical current density of the superconducting niobium film. The behavior of the critical current of a junction as a function of the parallel magnetic field is discussed for Abrikosov vortices of various types.

1. INTRODUCTION

It has now been established that Abrikosov vortices pinned in the electrodes of Josephson junctions have a strong effect on the physical properties of these junctions. In the first place, the pinned vortices near the junction increase the quasiparticle current by virtue of their normal cores.¹⁻⁴ This effect has been used to study the distribution of pinned vortices near the junction. The experimental data have been used to estimate the critical current density for a lead film.⁴ In Ref. 5, measurements of the quasiparticle current of several junctions in various regions of a superconducting film were used to study the spatial distribution of the pinned magnetic flux. Second, the pinned vortices suppress the Josephson critical current I_c of the junction because of their local magnetic field.^{4,6} This field causes additional spatial variation of the phase difference φ (Ref. 3).

Josephson junctions with both low and high numbers of vortices were studied in Refs. 3, 4, and 6–14. The suppression of the critical current of junctions with a small number of pinned vortices was studied in Refs. 7–12. Numerical calculations were carried out in Ref. 7 on the behavior $I_c(H_\perp)$ and $I_c(H_\parallel)$, where H_\perp and H_\parallel are magnetic fields directed perpendicular and parallel to the plane of the junction, for the case in which single Abrikosov vortices were pinned at the junction. The $I_c(H_\parallel)$ curves were used to determine the configuration and position of single vortices. This method was used to detect the motion of single vortices under the influence of the transport current and to estimate the elementary pinning force.⁹ The positions of single vortices pinned in the electrodes of a Josephson junction were observed directly by means of a low-temperature scanning electron microscope in Ref. 11. The experimental data yielded a distribution of the magnetic field lines from the vortices in the plane of the tunnel barrier. The motion of vortices under the influence of a transport current was visualized with the help of a low-temperature scanning electron microscope in Ref. 12, and the pinning force was measured.

The pinning of a large number of Abrikosov vortices was studied experimentally in Ref. 4. The behavior of I_c as a function of the vortex concentration was found there. The dependence of I_c on the vortex concentration was calculated in Ref. 13 for the case of a uniform distribution of mis-

matched vortices over the plane of the junction (Fig. 1a; a “mismatched” vortex penetrates both films of the junction, but the axes passing through the centers of the normal cores do not coincide³).

The usual way to pin vortices is to cool the junction from $T > T_c$ to $T < T_c$ in a magnetic field H_\perp (T_c is the superconducting transition temperature of the banks; this process is called “field cooling”). In this case the vortices are distributed uniformly over the plane of the junction, and the probability for the pinning of mismatched vortices is at its highest. The penetration of vortices into a niobium film was studied with the help of a Josephson junction in Ref. 14 during the application of a field H_\perp at $T < T_c$ (“zero-field cooling”). The configuration of the junction in Ref. 14 was such that isolated vortices penetrated into only the lower film (i.e., isolated vortices were pinned; Fig. 2a). We thus see that definite distributions of magnetic vortices near the Josephson junction can be produced by pinning the magnetic flux in various ways.

It can be concluded from this brief review of work on the effect of Abrikosov vortices on the properties of Josephson junctions that a question which remains relatively obscure is the effect of a large number of vortices on the critical current of a junction. In Sec. 2 we accordingly derive a theory for the critical Josephson current for Josephson junctions with large numbers of Abrikosov vortices of various types, distributed in various ways over the junction region. In Sec. 3 we report an experimental study of the effect of vortices on the critical current of a Josephson junction with niobium

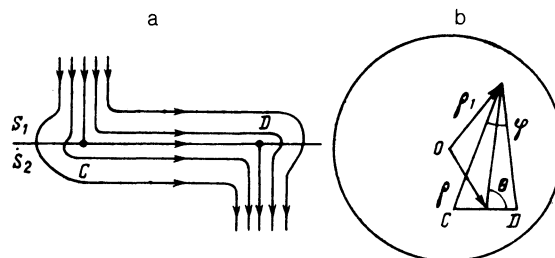


FIG. 1. a—Magnetic field distribution near a mismatched Abrikosov vortex in a Josephson junction ($CD = a$); b—determination of the spatial distribution of the phase difference φ for a mismatched vortex.

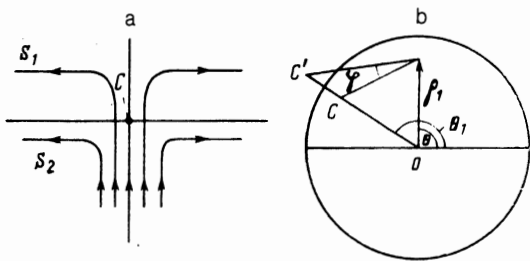


FIG. 2. a—Determination of the magnetic field near a single vortex in the lower film of the Josephson junction; b—determination of the $\varphi(\rho)$ dependence for a single vortex ($CC' = 2x$).

electrodes. Various methods were used to pin a large number of vortices in order to arrange conditions corresponding to the theoretical model of Sec. 3. The experimental results are discussed and compared with the theoretical results in Sec. 4.

2. CALCULATION OF THE CRITICAL CURRENT OF JOSEPHSON JUNCTIONS WITH ABRIKOSOV VORTICES OF VARIOUS TYPES

We assume that a small Josephson junction (with a size $L < \lambda_j$, where λ_j is the Josephson penetration depth) is in an external magnetic field \mathbf{H} directed parallel to the plane of the junction. We assume that N vortices are pinned in the junction. The critical current is found from

$$I_c^2 = j_0^2 \left| \int d^2\rho \exp[i\varphi(\rho)] \right|^2, \quad (1)$$

where j_0 is the critical current density in the absence of vortices, in a zero magnetic field (j_0 is determined by the properties of the tunnel barrier), and the integration is over the entire area of the junction. The phase difference φ depends on the external field and on the coordinates $\rho_i = (x_i, y_i)$ of the vortex in the junction:

$$\varphi = \sum_{i=1}^N \varphi(\rho - \rho_i) + \frac{2\pi\Phi x}{\Phi_0 L}, \quad (2)$$

where $\Phi = 2HL\lambda$, Φ_0 is the flux quantum, and $\varphi(\rho)$ is the phase shift caused by the local magnetic field of the vortex. To find the average junction current $\overline{I_c^2}$, we average expression (1) over various positions of the Abrikosov vortices:

$$\overline{I_c^2} = j_0^2 \int d^2\rho_1 \int d^2\rho_2 \exp\left[i \frac{2\pi\Phi}{\Phi_0 L} (x_1 - x_2)\right] \left\{ \int d^2\rho \frac{n(\rho)}{N} \times \exp[i\varphi(\rho_1 - \rho) - i\varphi(\rho_2 - \rho)] \right\}^N, \quad (3)$$

where $n(\rho)$ is the concentration of Abrikosov vortices, a function of the positions of these vortices.

To pursue the transformation of (3), we need to specify the function $\varphi(\rho)$ for various types of vortices. As we will see below, the phase shift caused by the presence of the vortex is small in most cases, and we can rewrite (3) as

$$\overline{I_c^2} = j_0^2 \int d^2\rho_1 \int d^2\rho_2 \exp\left[i \frac{2\pi\Phi}{\Phi_0 L} (x_1 - x_2) + \int d^2\rho n(\rho) \times \left\{ \exp[i\varphi(\rho_1 - \rho) - i\varphi(\rho_2 - \rho)] - 1 \right\}\right]. \quad (4)$$

Let us examine the suppression of the critical current of a Josephson junction for Abrikosov vortices of various types.

a) *Uniform distribution of mismatched Abrikosov vortices* (Fig. 1a). In this case the concentration of vortices is constant [$n(\rho) = n$], and the dependence of the phase difference on the coordinates of the vortices is as found in Refs. 3 and 13:

$$\sin \varphi = \frac{ap \sin \theta}{[(p^2 - a^2/4)^2 + a^2 p^2 \sin^2 \theta]^{1/2}}, \quad p = |\rho - \rho_1|. \quad (5)$$

Here a is the distance between the points at which a mismatched vortex enters and leaves the Josephson junction (Fig. 1b). Substituting the expression for the phase into (4), we can write the critical current as

$$\overline{I_c^2} = j_0^2 \int d^2\rho_1 \int d^2\rho_2 f(|\rho_1 - \rho_2|) \exp\left[i \frac{2\pi\Phi}{\Phi_0 L} (x_1 - x_2)\right], \quad (6)$$

$$f(z) = \begin{cases} (a/z)^\gamma, & z \gg a \\ 1, & z \ll a \end{cases}, \quad \gamma = \pi n a^2.$$

In deriving (6) we noted that at low vortex concentrations the current is dominated by those values of ρ_1 and ρ_2 which satisfy $|\rho_1 - \rho_2| \gg a$.

Assuming that the sample is a disk of radius L , we can put (6) in the following form (we are using Fourier transforms):

$$\overline{I_c^2} = j_0^2 (2\pi)^2 L^2 \int \frac{dq}{q} J_1^2(qL) J_0(qx) \int x f(x) J_0\left(\frac{2\pi\Phi x}{\Phi_0 L}\right) dx, \quad (7)$$

where $J_1(z)$ and $J_0(z)$ are Bessel functions.

We rewrite (7) as

$$\overline{I_c^2} = 8\pi L^4 j_0^2 \int_0^1 dt (1-t^2)^{1/2} \int_0^{2t} x f(xL) J_0\left(\frac{2\pi\Phi x}{\Phi_0}\right) dx. \quad (8)$$

At low concentrations, $\gamma \ll 1$, the optimum values of x are much greater than a , and we can rewrite (8) as

$$\overline{I_c^2} = 8\pi L^4 j_0^2 \left(\frac{a}{L}\right)^\gamma \int_0^1 dt (1-t^2)^{1/2} \int_0^{2t} x^{1-\gamma} J_0\left(\frac{2\pi\Phi x}{\Phi_0}\right) dx. \quad (9)$$

In weak magnetic fields ($\Phi/\Phi_0 \ll 1$) the Bessel function can be replaced by unity, and we find

$$\overline{I_c^2} = j_0^2 \frac{(8\pi)^{1/2}}{2-\gamma} L^4 \left(\frac{a}{2L}\right)^\gamma \frac{\Gamma(3/2-\gamma/2)}{\Gamma(3-\gamma)}. \quad (10)$$

In the opposite case of high magnetic fields ($\Phi/\Phi_0 \gg 1$), we find the following expression, making use of the asymptotic expression for the Bessel function at large values of its argument:

$$\overline{I_c^2} = 8\pi L^4 j_0^2 \left(\frac{a}{2L}\right)^\gamma \left\{ \frac{\gamma\pi}{4} \frac{\Gamma(1-\gamma/2)}{\Gamma(1+\gamma/2)\alpha^{2-\gamma}} + \frac{1}{\alpha^2} \left[\frac{\Gamma(3/2-\gamma/2)}{\Gamma(1/2+\gamma/2)\alpha^{-1}} - \frac{\sin 2\alpha}{2} \right] \right\}, \quad (11)$$

where $\alpha = 2\pi\Phi/\Phi_0$. The first term in (11) describes the deviation from "Fraunhofer" dependence due to fluctuations of the Josephson phase in the junction. This deviation

is small at small values of γ , and it decreases with increasing magnetic field (in contrast with the constant "pedestal" which arises from fluctuations of the critical current density). The critical current in the region of nonvanishing magnetic fields behaves nonmonotonically with increasing vortex concentration (in contrast with the current at $H = 0$): At $\gamma = a/2L \ll 1$, the current reaches a maximum value. For $\gamma \ll 1$, the amplitude of the oscillations on the $\bar{I}_c(\Phi)$ curve is small. However, on the typical $I_c(\Phi)$ curve we should see random oscillations with a period $\sim \Phi_0$ and an amplitude $\sim \bar{I}_c$. The reason lies in the pronounced fluctuations from sample to sample in the critical currents of junctions with vortices (the "mesoscopic" behavior of a Josephson junction¹⁵).

At high vortex concentrations ($\gamma \gg 1$), expression (8) is dominated by the region $x \approx a$, and the critical current becomes independent of n .

b) *Isolated vortices distributed in a narrow region near the boundary of the superconductors (Fig. 2, a and b).* The change in the Josephson phase due to the presence of isolated vortices is given by (we are assuming that the sample is a disk of radius L)

$$\varphi = \frac{2x\rho_1 \sin(\theta_1 - \theta)}{\rho_1^2 + L^2 - 2\rho_1 L \cos(\theta_1 - \theta)}, \quad (12)$$

where x is the distance from the vortex entry point to the boundary of the sample, and the angles θ_1 and θ are explained in Fig. 2b. Substituting (12) into (4), and introducing the dimensionless quantities $t = \rho/L$, $t_1 = \rho_1/L$, and $t_2 = \rho_2/L$, we find

$$\begin{aligned} \bar{I}_c^2 = j_0^2 L^4 \int_0^1 t_1 dt_1 \int_0^1 t_2 dt_2 \int_0^{2\pi} d\theta_1 \int_0^{2\pi} d\theta_2 \\ \times \exp \left\{ i \frac{2\pi\Phi}{\Phi_0 L} (t_1 \cos \theta_1 - t_2 \cos \theta_2) \right. \\ \left. + \pi L^4 \int_0^1 t n(tL) (1-t)^2 dt \int_0^{2\pi} d\theta \left[\frac{t_1 \sin(\theta_1 - \theta)}{t_1^2 - 2t_1 \cos(\theta_1 - \theta) + 1} \right. \right. \\ \left. \left. - \frac{t_2 \sin(\theta_2 - \theta)}{t_2^2 - 2t_2 \cos(\theta_2 - \theta) + 1} \right] \right\}. \quad (13) \end{aligned}$$

For isolated vortices distributed in a narrow region near the boundary, the critical current thus depends on the quantity

$$Z = \pi L^4 \int_0^1 t n(tL) (1-t)^2 dt.$$

If we have $Z \ll 1$, the second term in the argument of the exponential function is small. Carrying out a series expansion we find in weak magnetic fields ($\Phi/\Phi_0 \ll 1$)

$$\bar{I}_c^2 = j_0^2 \pi^2 L^4 (1 - \alpha_1 Z), \quad (14)$$

where the coefficient α_1 is on the order of unity.

In strong magnetic fields $\Phi/\Phi_0 \gg 1$ with $Z \ll 1$, the magnetic-field dependence of the critical current differs only slightly from Fraunhofer dependence. A pedestal appears on the $I_c(H)$ curve with a magnitude proportional to Z .

At a high vortex concentration ($Z \gg 1$), the current is dominated by approximately equal values of t_1 and t_2 —val-

ues satisfying $|t_1 - t_2| \ll 1$. Expression (13) can then be rewritten as

$$\begin{aligned} \bar{I}_c^2 = 2\pi j_0^2 L^4 \int_0^1 t_1 dt_1 \int_{-\infty}^{\infty} dt_x dt_y \exp \left[i \frac{2\pi\Phi}{\Phi_0} t_x - \alpha_2 Z (t_x^2 + t_y^2) \right], \\ \alpha_2 = \int_0^{2\pi} d\theta \frac{(t_1^2 - 1)^2 \sin^2 \theta}{(t_1^2 - 2t_1 \cos \theta + 1)^4} \approx 1. \quad (15) \end{aligned}$$

Here we have used $t_1 \sim 1$. Evaluating the integrals in (15), we find

$$\bar{I}_c^2 = \frac{\pi^2 j_0^2 L^4}{Z \alpha_2} \exp \left[- \left(\frac{\pi\Phi}{\Phi_0} \right)^2 \frac{1}{\alpha_2 Z} \right]. \quad (16)$$

It can be seen from (16) that the oscillations disappear from the $I_c(H)$ curve if the concentration of vortices in the narrow region near the boundary (the distance to which the vortices penetrate is $b \ll L$) is high ($Z \gg 1$).

3. EXPERIMENTAL PROCEDURE AND RESULTS

3.1. *Test samples and experimental apparatus.* The experiments were carried out on an Nb-AlO_x-Nb Josephson junction of the *S-I-S* type, fabricated by selective anodizing of the niobium.¹⁶ To arrange conditions such that isolated vortices would penetrate into the lower electrode alone during the application of a field H_1 at $T < T_c$, we prepared some island samples with peripheral regions surrounding the tunnel junction in both the lower and upper electrodes. The lower region was larger than the upper one. We studied two samples, with similar configurations (samples 1 and 2). The characteristics of junction 1 and some of the results found on it were published in Ref. 14. In the present paper we are reporting the characteristics of junction 2 and the experimental results obtained on this sample alone.

Figure 3 shows the configuration of junction 2 (this is a top view). In this configuration, the lower electrode screens the perpendicular magnetic field out of the upper electrode by virtue of the Meissner effect. The size of the region in junction 2 is $9 \times 9 \mu\text{m}^2$. The thicknesses of the lower and upper electrodes in the junction region are $\approx 0.27 \mu\text{m}$ and $\approx 0.53 \mu\text{m}$, respectively. At $T = 4.2 \text{ K}$, the (doubled) London penetration depth is $2\lambda_L \approx 0.25 \mu\text{m}$ (as estimated from the $I_c(H_{\parallel})$ curve¹⁷). This junction falls in the category of small junctions with a Josephson penetration depth

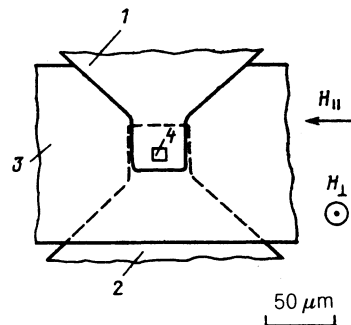


FIG. 3. Configuration of the Josephson junction (top view). The orientations of the magnetic fields applied in the course of the experiments are indicated. 1)—Nb upper electrode; 2)—Nb lower electrode; 3)—SiO₂ insulating layer; 4)—J_{jct}

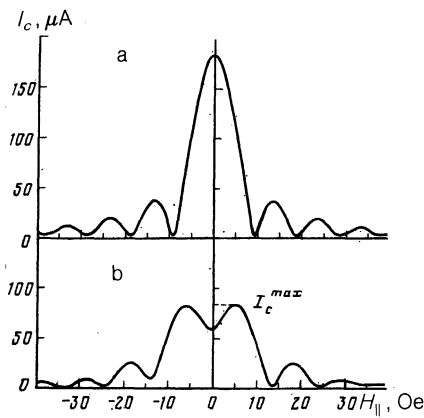


FIG. 4. a— $I_c(H_{\parallel})$ curve measured for a Josephson junction in whose electrodes there are no pinned Abrikosov vortices; b— $I_c(H_{\parallel})$ measured after a junction was cooled in a perpendicular magnetic field $H_{\perp} = 0.14$ Oe. The dashed line shows the maximum critical current I_c^{\max} .

$\lambda_j(T = 4.2 \text{ K}) \approx 22 \text{ } \mu\text{m}$. The superconducting transition temperature is $T_c = 8.9 \pm 0.1 \text{ K}$ for both electrodes.

The sample was held in a cell filled with helium as a heat-exchange gas, so a thermal cycling could be carried out with a controllable cooling rate. Magnetic fields were applied in the directions perpendicular and parallel to the plane of the junction by means of copper coils. The geomagnetic field was screened out by a shield made of Permalloy (the residual field was $\leq 0.01 \text{ G}$). The critical Josephson current was measured by a computer-controlled device with an operating time $\sim 0.1 \text{ s}$ and an absolute error of $2 \text{ } \mu\text{A}$.

3.2. *Introduction of Abrikosov vortices during cooling of the Josephson junction in a perpendicular magnetic field.* The experimental cycle consisted of the following steps.

- 1) The sample was heated to $T > T_c$.
- 2) A perpendicular magnetic field H_{\perp} of fixed strength was applied.
- 3) The junction was cooled slowly in the perpendicular field H_{\perp} to $T = 4.2 \text{ K}$.
- 4) The field H_{\perp} was turned off.
- 5) The $I_c(H_{\parallel})$ curve was measured at $T = 4.2 \text{ K}$.

Figure 4a shows an $I_c(H_{\parallel})$ curve measured after the junction was cooled in a zero magnetic field H_{\perp} ; magnetic flux was pinned in the electrodes of this junction. This curve is approximately an ideal Fraunhofer curve, implying a uniform distribution of the critical current density over the cross section of the junction.

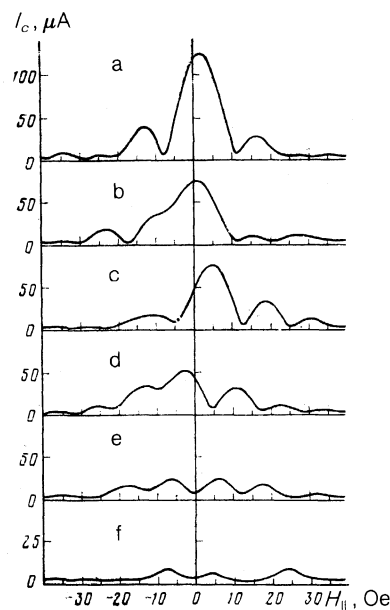


FIG. 5. $I_c(H_{\parallel})$ curves measured after a junction was cooled in perpendicular magnetic fields H_{\perp} of various strengths. a— $H_{\perp} = 0.9 \text{ Oe}$; b—2.2; c—3.0; d—3.9; e—6.5; f—8.3.

The deviation of $I_c(H_{\parallel})$ from a “vortex-free” Fraunhofer curve became detectable starting at a cooling field $H_{\perp} \approx 0.04 \text{ Oe}$. As in Refs. 7 and 10, we found that when the field H_{\perp} was raised further, in steps of $\approx 0.02 \text{ G}$ to $H_{\perp} \approx 0.4 \text{ G}$, the dependence of I_c^{\max} on the cooling field had steps. Each step on the given curve corresponded to a certain type of $I_c(H_{\parallel})$ curve, different from a vortex-free curve. Figure 4b shows $I_c(H_{\parallel})$ measured after the sample was cooled in a magnetic field $H_{\parallel} = 0.14 \text{ Oe}$. Here we see some substantial differences from the curve in Fig. 4a (the dashed line shows I_c^{\max}). According to Refs. 7–10, these deviations from a Fraunhofer curve indicate pinning of Abrikosov vortices near the junction.

Cooling in fields $H_{\perp} > 0.4 \text{ Oe}$ resulted in even greater deviations of the $I_c(H_{\parallel})$ curve from a Fraunhofer curve. Figure 5, a–f, shows some representative $I_c(H_{\parallel})$ curves measured in fields $H_{\perp} > 0.4 \text{ Oe}$. On these curves we see that I_c^{\max} appears as the cooling field is raised. We see oscillations in I_c with a period Φ_0 . The main and side maxima move closer together. From the $I_c(H_{\parallel})$ curves we found values of I_c^{\max} corresponding to different values of the cooling field H_{\perp} , and we plotted $I_c^{\max}(H_{\perp})$. The result is shown in Fig. 6a.

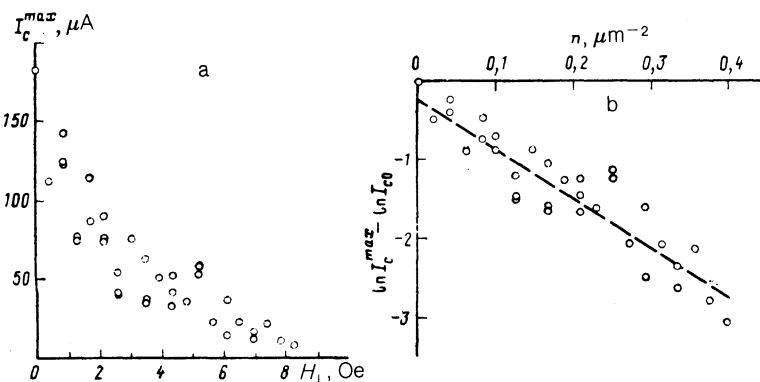


FIG. 6. a— I_c^{\max} versus the strength of the perpendicular magnetic field H_{\perp} in which the junction was cooled (the method for determining I_c^{\max} is explained in Fig. 4b); b—curve of $\ln I_c^{\max} - \ln I_{c0}$ versus n (the concentration of vortices pinned in the junction region) constructed from the data in Fig. 6a. The dashed line is a linear approximating function. The parameters of this function were found by the method of least squares.

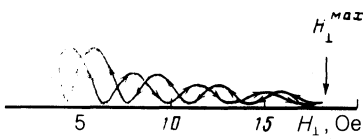


FIG. 7. Direct experimental recording of a $I_c(H_{\perp})$ curve with hysteresis, illustrating the introduction of vortices by the second method. Here H_{\perp}^{\max} is the maximum strength of the perpendicular magnetic field reached in the given measurement cycle ($H_{\perp}^{\max} = 18.3$ Oe), and $T = 4.2$ K.

We see that the $I_c^{\max}(H_{\perp})$ curve has the characteristic downward-concave shape.

3.3. *Vortex penetration into the junction during the application of a perpendicular magnetic field at $T < T_c$. The experiments in which the vortices were introduced into the junction by the second method consisted of the following steps.*

1) The sample was heated to $T > T_c$.

2) The junction was cooled in a zero magnetic field (the fields both parallel and perpendicular to the plane of the junction were zero) to $T = 4.2$ K.

3) The field H_{\perp} was increased from zero to a certain H_{\perp}^{\max} and then reduced to zero. At the same time, the critical

current I_c was measured [i.e., $I_c(H_{\perp})$ curves were recorded].

4) The curve of $I_c(H_{\parallel})$ was recorded.

Each successive measurement cycle began with heating of the junction to $T > T_c$ and cooling of the junction to $T = 4.2$ K in a zero magnetic field. As in Ref. 14, we found that for $H_{\perp}^{\max} < H_{\perp}^*$ the $I_c(H_{\perp})$ curves had no hysteresis, and the $I_c(H_{\parallel})$ curves had basically the same shape as the vortex-free curve shown in Fig. 4a. At fields $H_{\perp}^{\max} \geq H_{\perp}^*$, however, hysteresis appeared on the $I_c(H_{\perp})$ curve (Fig. 7), and distortion appeared in the $I_c(H_{\parallel})$ curves. Specifically, the maximum critical Josephson current decreased, and the size of the side maxima also changed. For sample 2 we found $H_{\perp}^* = 7$ Oe. Figure 8, a-g, shows several $I_c(H_{\parallel})$ curves measured at various values of H_{\perp}^{\max} . It can be seen from these results that, in contrast with the previous experiments on the pinning of Abrikosov vortices by cooling through T_c , the $I_c(H_{\parallel})$ curves are qualitatively similar to a Fraunhofer curve even when there is a substantial suppression of the current I_c^{\max} . From a set of $I_c(H_{\parallel})$ curves measured for various magnetic fields H_{\perp}^{\max} we constructed $I_c^{\max}(H_{\perp}^{\max})$; the result is shown in Fig. 9a. In the region from zero to H_{\perp}^* on this curve there is no substantial change in the value of I_c^{\max} .

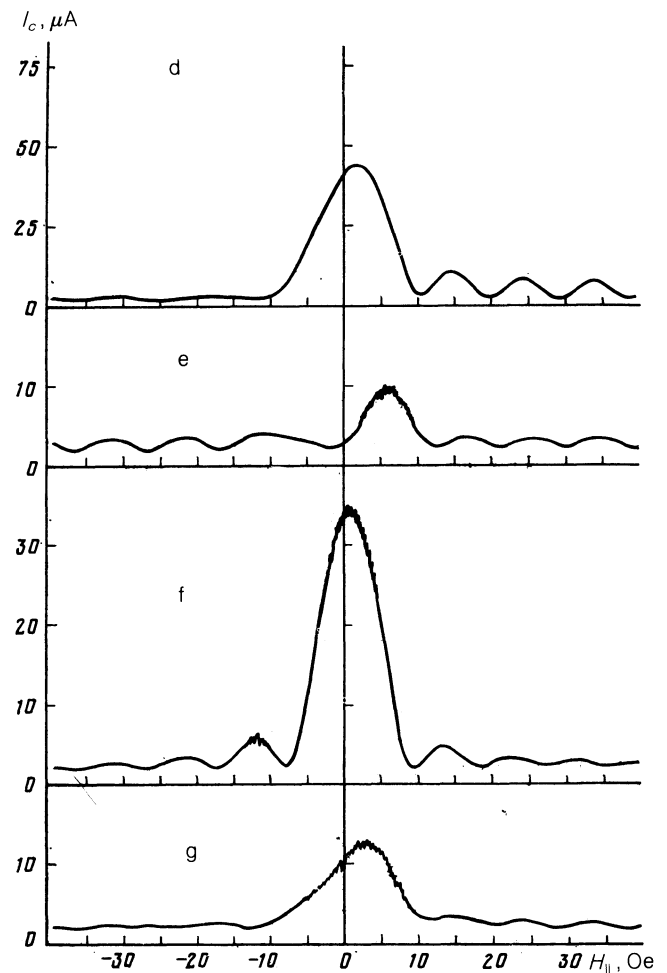
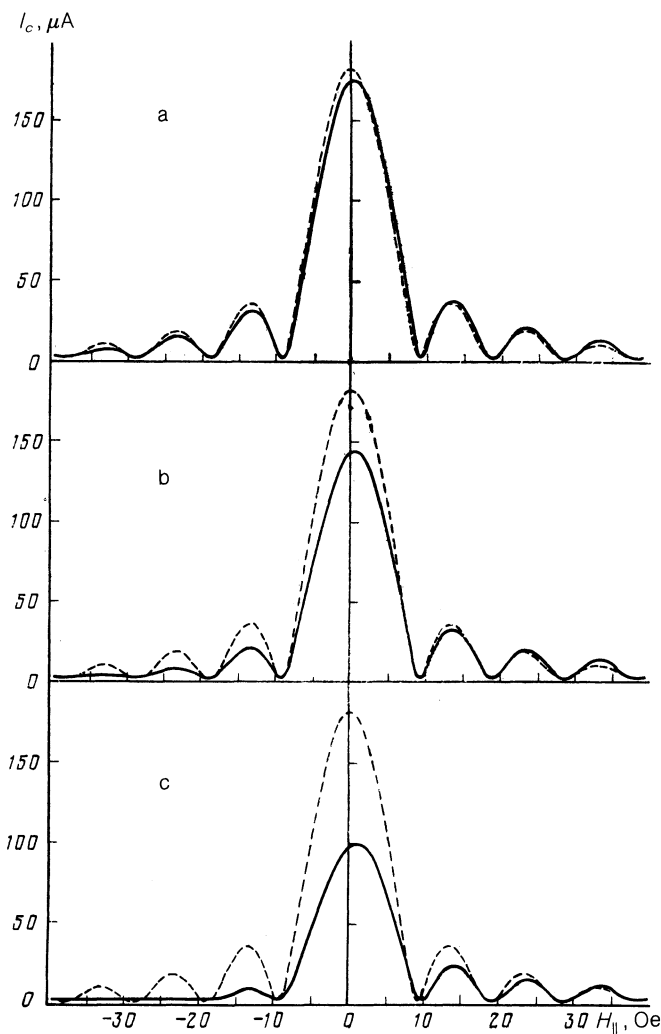


FIG. 8. Curves of $I_c(H_{\parallel})$ measured after the application of magnetic fields H_{\perp}^{\max} of various strengths during the introduction of vortices by the second method. a— $H_{\perp}^{\max} = 15.7$ Oe; b—18.3; c—20.1; d—21.9; e—23.6; f—25.3; g—27.9. $T = 4.2$ K. The dashed line shows a vortex-free curve $I_c(H_{\parallel})$.

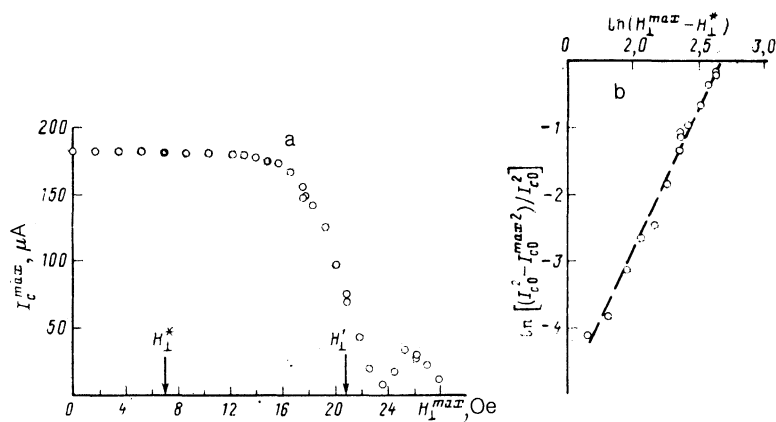


FIG. 9. a: $I_c^{\max}(H_1^{\max})$. The value of I_c^{\max} was found from the $I_c(H_{\parallel})$ curves measured after the application of magnetic fields H_1^{\max} of various strengths. b: $\ln[(I_{c0}^2 - I_c^{\max 2})/I_{c0}^2]$ versus $\ln(H_1^{\max} - H_1^*)$ as constructed from the experimental data on $I_c^{\max}(H_1^{\max})$ in Fig. 9a, over the magnetic-field interval H_1^{\max} 12.2-20.9 Oe. The dashed line shows an approximating straight line; the coefficients of this line were found by the method of least squares.

At H_1^* , the value of I_c^{\max} begins to decrease smoothly. The curve of $I_c^{\max}(H_1^{\max})$ is convex upward (in contrast with the curve in Fig. 6a, with an inflection point at $H_1^{\max} - H_1' = 20.9$ Oe, beyond which the curve is convex downward). In the magnetic-field interval $H_1 = 23.6 + 27.9$ Oe, the curve of $I_c^{\max}(H_1^{\max})$ has a clearly defined peak [the $I_c(H_{\parallel})$ curve corresponding to the crest of this peak is shown in Fig. 8f].

In concluding this discussion of the experimental part of the study, we note that results similar to those described above were found for sample 1. When Abrikosov vortices are pinned in junction 1 by the first method, the curves of $I_c(H_{\parallel})$ measured at various fields H_1 deviate substantially from the vortex-free Fraunhofer curve, and the curve of $I_c^{\max}(H_1)$ has the characteristic downward-concave shape. These results are the same as those found for junction 2. When the vortices are introduced by the second method, we find curves of $I_c(H_{\parallel})$ for junction 1 (as for junction 2) which exhibit a progressively greater deviation from the vortex-free shape with increasing $H_1^{\max}H_1^*$. The $I_c^{\max}(H_1^{\max})$ dependence is qualitatively the same as shown in Fig. 9a, and the shape of the $I_c(H_{\parallel})$ curves at $H_1^{\max} > H_1'$ is the same for both samples.

4. DISCUSSION OF RESULTS

4.1. Suppression of the critical Josephson current during the introduction of vortices by the two methods. We begin with a discussion of the results on the pinning of vortices during cooling through T_c in the presence of a magnetic field. When the flux is pinned by cooling through T_c , vortices can form in both the upper and lower films. The niobium films from which the junction was fabricated had a granular structure. The grain boundaries were the most probable sites for a pinning of vortices. It follows that the uniform distribution of pinning centers over the film led to a uniform spatial distribution of the vortices over the junction region in the case of cooling through T_c in a magnetic field.

The formation of the first (single) Abrikosov vortex on the area of the junction during cooling through T_c requires a magnetic field $H_1^{\text{cr}} = \Phi_0/S \approx 0.25$ Oe (S is the area of the junction).⁷ Cooling in a field $H_1 \sim H_1^{\text{cr}}$ thus led to the pinning of approximately one vortex. Further evidence for this conclusion comes from the characteristic shape of the measured $I_c(H_{\parallel})$ curves, which is different from the shape of the Fraunhofer curve.¹⁰ For example, the curve in Fig. 4b corre-

sponds to the situation in which an isolated vortex is in the central part of the junction. During cooling through T_c , mismatched Abrikosov vortices may also be pinned (Fig. 1b). However, when the number of vortices in the junction region is small, isolated vortices dominate the suppression of I_c^{\max} and the distortion of the $I_c(H_{\parallel})$ curve (Fig. 2b).

During cooling through T_c in magnetic fields $H_1 \gg H_1^{\text{cr}}$, a large number of mismatched vortices are pinned (since vortices can be pinned in both the upper and lower films of the junction). Because of the uniform distribution of pinning centers over the junction region, the spatial distribution of vortices is also uniform. We can thus use the model of a uniform distribution of mismatched Abrikosov vortices (Fig. 1b) over the junction area to explain the experimental results obtained on the pinning of vortices in strong magnetic fields by the first method (Sec. 2). Under the condition $\pi na^2 \ll 1$, we can rewrite (10) as

$$\ln I_c^{\max} - \ln I_{c0} = n \frac{\pi a^2}{2} \ln \frac{a}{2L}, \quad (17)$$

where I_{c0} is the critical Josephson current in the absence of an H_{\parallel} field. The equations in Sec. 2 correspond to the case of cylindrical geometry. In the experiments, in contrast, we studied junctions of square geometry. We accordingly take L to be the radius of a circular Josephson junction with an area equal to $9 \times 9 \mu\text{m}^2$. Figure 6b shows $\ln I_c^{\max} - \ln I_{c0}$ versus the vortex concentration n found by modifying the $I_c^{\max}(H_1)$ curve (Fig. 6a). The concentration n was found from the formula $n = H_1 S / \Phi_0$. We see that the modified dependence of $\ln I_c^{\max} - \ln I_{c0}$ on n can be approximated satisfactorily by a linear function $f(n) = dn + k$ (the dashed line in Fig. 6b). This result corresponds to the model for the suppression of the critical current I_c^{\max} by pinning of a large number of mismatched vortices distributed uniformly over the junction region. From (17) we find $d = (\pi a^2/2) \ln(a/2L)$. From this expression we find an estimate $\sim 1 \mu\text{m}$ for a . By way of comparison, the mismatch parameter for Sn-Sn_xO_y-Sn junction, of the $S-I-S$ type, is $\sim 0.3 \mu\text{m}$, while that for $S-N-S$ Pb(2.5% Bi)-Ag(4% Al)-Pb(2.5% Bi) junctions is $\sim 10 \mu\text{m}$ (Ref. 7). The large scatter in the values of I_c^{\max} at the various values of H_1 is a consequence of fluctuations in both the actual number of vortices pinned in the film and the positions of these vortices.

When vortices are introduced by the second method, the vortices can penetrate into only the low-

er film, because of the screening of the upper electrode by the lower one (Fig. 3). When a field $H_{\perp}^{\max} = H_{\perp}^*$ is reached, the isolated vortices which have gone into the lower film begin to penetrate into the junction from its edges; as H_{\perp}^{\max} is raised further, these vortices penetrate progressively further into the junction.¹⁴ This method thus results in the introduction of primarily isolated vortices into the junction region (Fig. 2b), and the theory derived in Subsection (2.2) can be used to interpret the experimental results. In the critical-state model the dependence of the vortex concentration on the distance is written in the form¹⁸

$$n(x) = \frac{B(x)}{\Phi_0} = \begin{cases} \beta(x-L+b)^m/\Phi_0, & x \geq L-b \\ 0, & x < L-b \end{cases}, \quad (18)$$

where $B(x)$ is the magnetic induction at the point x , and the parameters β and m depend on the particular model selected. For the Bean model we would have $m = 1$ and $\beta = 4\pi j_c/c$, where j_c is the critical current density of the superconducting film. For the Kim-Anderson model we would have $m = 1/2$, and β would be determined by the pinning force. The distance to which the vortices penetrate depends on the actual value of the field at the junction boundary, B_{\perp}^p :

$$b = \left[\frac{B_{\perp}^p}{\beta} \right]^{1/m} = \left[\frac{(H_{\perp}^{\max} - H_{\perp}^*)r}{\beta} \right]^{1/m}, \quad (19)$$

where r is the demagnetizing factor, and H_{\perp}^{\max} is the magnetic field in the absence of the junction. If we have $b \ll L$, the H_{\perp}^{\max} dependence of the critical current I_c can be written as follows, according to (14) and (16):

$$(I_c^{\max})^2 = I_{c0}^2 \{1 - f[r(H_{\perp}^{\max} - H_{\perp}^*)]^{(3+m)/m}\},$$

$$f[r(H_{\perp}^{\max} - H_{\perp}^*)]^{(3+m)/m} \ll 1, \quad (20)$$

$$(I_c^{\max})^2 = I_{c0}^2 \left\{ \frac{\alpha_1}{\alpha_2 f[r(H_{\perp}^{\max} - H_{\perp}^*)]^{(3+m)/m}} \right\},$$

$$f[r(H_{\perp}^{\max} - H_{\perp}^*)]^{(3+m)/m} \gg 1, \quad (21)$$

$$f = \frac{8\pi\alpha_1\Gamma(m+1)}{L\Phi_0\Gamma(m+4)\beta^3}.$$

For the lower film, into which the vortices penetrate, the demagnetizing coefficient is¹⁹ $r \approx 80$. Figure 9b shows a curve of $I_c^{\max}(H_{\perp}^{\max})$ reconstructed over the magnetic-field interval 12.2–20.9 Oe, in the coordinates $\ln[(I_{c0}^2 - I_c^{\max 2})/I_{c0}^2]$, $\ln(H_{\perp}^{\max} - H_{\perp}^*)$. This curve can be approximated quite accurately by a linear function (the dashed line). Working from the parameter values of the linear function, we determined the constant m and estimated the critical current density j_c of the niobium film. We found $m \approx 1$. This value corresponds to a description of the penetration of vortices into the film of the junction as in the Bean model. The estimate of j_c yielded $3.10^7 - 5.10^7$ A/cm², which agrees satisfactorily with independent measurements of j_c which have been carried out previously²⁰ by a direct method for similar niobium films.

Analysis of the experimental data for fields $H_{\perp} > H_{\perp}^*$ shows that the $I_c^{\max}(H_{\perp}^{\max})$ curve can be described by the formula $I_c \propto \exp(-\alpha H_{\perp}^{\max})$. In other words, the decrease in I_c^{\max} with increasing H_{\perp}^{\max} is far steeper than would follow

from (16) and (21). The apparent reason for this result is the violation of the condition $b \ll L$ as isolated vortices penetrate into the junction in fields $H_{\perp} \gg H_{\perp}^*$ (the suppression of the critical Josephson current ΔI_c from each individual vortex which has penetrated a distance $b \sim L$ into the junction is very strong,³ $\Delta I_c/I_{c0} \approx 1$).

One might suggest that at $H_{\perp}^{\max} = 23.6$ Oe the entire junction region is filled with single vortices and that the peak on the $I_c^{\max}(H_{\perp}^{\max})$ curve at $H_{\perp}^{\max} = 25.3$ Oe is apparently a result of a mutual cancellation of the magnetic fields of the vortices (at $H_{\perp}^{\max} > 25.3$ Oe, the cancellation conditions are disrupted, and I_c^{\max} decreases).

4.2. Distortions of the $I_c(H_{\parallel})$ curve as a result of the pinning of Abrikosov vortices in different ways. The type of vortex and the distribution of vortices in the Josephson junction also affect the $I_c(H_{\parallel})$ dependence. In a situation involving the pinning of only a few vortices, it is possible to make a quantitative comparison of the experimental $I_c(H_{\parallel})$ curves with the theoretical curves.⁷⁻¹⁰ If instead a large number of vortices are pinned—the case in which we are interested here—we can at best make a qualitative comparison of the experimental data with the predictions of the theoretical model.

When the flux is pinned as the junction is cooled through T_c in a perpendicular magnetic field, the experimental $I_c(H_{\parallel})$ curves differ greatly from the Fraunhofer curve (Fig. 5). We see that on the whole the critical current decreases smoothly with increasing strength of the parallel field. This result can be described quite well qualitatively by expression (11), which was derived from the condition for the pinning of mismatched vortices distributed uniformly over the junction area. On the measured $I_c(H_{\parallel})$ curves we also observed oscillations in the current I_c , with a period $\sim \Phi_0$ and an amplitude $\sim I_c^{\max}$. The value of I_c^{\max} was greatly reduced. Oscillations of this sort can be linked with the mesoscopic behavior of a disordered Josephson junction.¹⁵

When the vortices were introduced by the second method, individual vortices were pinned in the lower film. In the weak-field region ($H_{\perp}^{\max} < H_{\perp}^*$) the $I_c(H_{\parallel})$ curves differ only slightly from the Fraunhofer curve (Fig. 8), in agreement with expression (13). We might point out certain aspects of the $I_c(H_{\parallel})$ curves in magnetic fields $H_{\perp}^{\max} > H_{\perp}^*$: There is a clearly defined maximum in the current I_c , and the $I_c(H_{\parallel})$ dependence is asymmetric (the oscillations are retained at $H_{\parallel} > 0$, while the current decreases sharply at $H_{\parallel} < 0$; Fig. 8d). Again, the reason is the penetration of a large number of single vortices into the interior of the junction ($b \approx L$).

The results of this theoretical and experimental study thus show that one can work from such characteristics of a Josephson junction as the maximum Josephson current I_c^{\max} and the $I_c(H_{\parallel})$ dependence in the case of the pinning of a large number of Abrikosov vortices to reach conclusions about the configuration of vortices and their distribution over the junction area. The theoretical method which we have developed for calculating I_c^{\max} and $I_c(H_{\parallel})$ curves for various configurations and distributions of vortices leads to results which agree qualitatively and quantitatively with data from experiments in which vortices were introduced in various ways, and the situations were close to the model situations.

We wish to thank A. A. Abrikosov for a discussion of this study and A. S. Nigmatulin and F. N. Sklokin for assistance in organizing the experiments.

- ¹ W. T. Band and G. B. Donaldson, *J. Phys. F* **4**, 2017 (1974).
² T. A. Fulton, A. F. Hebard, L. N. Dunkleberger, and R. H. Eick, *Solid State Commun.* **22**, 493 (1977).
³ A. A. Golubov and M. Yu. Kupriyanov, *Zh. Eksp. Teor. Fiz.* **92**, 1512 (1987) [*Sov. Phys. JETP* **65**, 849 (1987)].
⁴ N. Uchida, K. Enpuku, Y. Matsugaki *et al.*, *J. Appl. Phys.* **54**, 5287 (1983).
⁵ N. Uchida, K. Enpuku, K. Yoshida, and F. Irie, *J. Appl. Phys.* **56**, 2558 (1984).
⁶ M. A. Washington and T. A. Fulton, *Appl. Phys. Lett.* **40**, 848 (1982).
⁷ S. Miller, K. R. Biagi, J. R. Clem, and D. K. Finnemore, *Phys. Rev. B* **31**, 2684 (1985).
⁸ O. V. Hyun, D. K. Finnemore, L. Schwartzkopf, and J. R. Clem, *Phys. Rev. Lett.* **58**, 599 (1987).
⁹ O. B. Hyun, J. R. Clem, L. A. Schwartzkopf, and D. K. Finnemore, *IEEE Trans. Magn.* **MAG-23**, 1176 (1987).
¹⁰ O. B. Hyun, J. R. Clem, and D. K. Finnemore, *Phys. Rev. B* **10**, 175 (1989).
¹¹ J. Mannhart, J. Bosch, R. Gross, and R. P. Huebener, *Phys. Rev. B* **35**, 5267 (1987).
¹² J. Mannhart, J. Bosch, R. Gross, and R. P. Huebener, *Phys. Lett. A* **122**, 139 (1987).
¹³ M. V. Fistul', *Pis'ma Zh. Eksp. Teor. Fiz.* **52**, 823 (1990) [*JETP Lett.* **52**, 192 (1990)].
¹⁴ V. N. Gubankov, M. P. Lisitskiĭ, I. L. Serpuchenko, and F. N. Sklokin, *Pis'ma Zh. Eksp. Teor. Fiz.* **51**, 630 (1990) [*JETP Lett.* **51**, 716 (1990)].
¹⁵ M. V. Fistul', *Zh. Eksp. Teor. Fiz.* **96**, 369 (1989) [*Sov. Phys. JETP* **69**, 209 (1989)].
¹⁶ An. B. Ermakov, V. P. Koshelets, S. A. Kovtonyuk *et al.*, in *Extended Abstracts, ISEC '89*, Tokyo, 1984, p. 294.
¹⁷ A. Barone and G. Paternò, *Physics and Applications of the Josephson Effect*, Wiley-Interscience, New York, 1981 (Russ. Transl. Mir, Moscow, 1986).
¹⁸ P. G. de Gennes, *Superconductivity of Metals and Alloys*, Benjamin, New York, 1966 (Russ. Transl. Mir, Moscow, 1968).
¹⁹ T. Van Duzer and O. Turner (editors), *Principles of Superconductive Devices and Circuits*, Elsevier, New York, 1981 (Russ. Transl. Radio i svyaz, Moscow, 1984).
²⁰ M. E. Gershenzon and V. N. Gubankov, *Fiz. Tverd. Tela (Leningrad)* **21**, 700 (1979) [*Sov. Phys. Solid State* **21**, 411 (1979)].

Translated by D. Parsons